

Amphiphilic Polymer Conetworks Based on End-Linked “Core-First” Star Block Copolymers: Structure Formation with Long-Range Order

Eleni J. Kepola,[†] Elena Loizou,[†] Costas S. Patrickios,^{*,†} Epameinondas Leontidis,[†] Chrysovalantis Voutouri,[‡] Triantafyllos Stylianopoulos,[‡] Ralf Schweins,[#] Michael Gradzielski,[§] Christian Krumm,^{||} Joerg C. Tiller,^{||} Michelle Kushnir,[⊥] and Chrys Wesdemiotis[⊥]

[†]Department of Chemistry and [‡]Department of Mechanical and Manufacturing Engineering, University of Cyprus, 1678 Nicosia, Cyprus

[#]Large Scale Structures Group, Institut Laue-Langevin, 71 Avenue des Martyrs, CS 20 156, Grenoble F-38042 Cedex 9, France

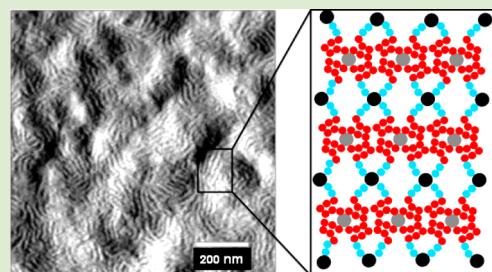
[§]Stranski-Laboratorium für Physikalische und Theoretische Chemie, Institut für Chemie, Technische Universität Berlin, D-10623 Berlin, Germany

^{||}Department of Biochemical and Chemical Engineering, Technische Universität Dortmund, D-44227 Dortmund, Germany

[⊥]Department of Chemistry and Integrated Biosciences Program, University of Akron, Akron, Ohio 44325-3601, United States

Supporting Information

ABSTRACT: Amphiphilic polymer conetworks are cross-linked polymers that swell both in water and in organic solvents and can phase separate on the nanoscale in the bulk or in selective solvents. To date, however, this phase separation has only been reported with short-range order, characterized by disordered morphologies. We now report the first example of amphiphilic polymer conetworks, based on end-linked “core-first” star block copolymers, that form a lamellar phase with long-range order. These mesoscopically ordered systems can be produced in a simple fashion and exhibit significantly improved mechanical properties.



Polymeric hydrogels consist mostly of water held in place by a hydrophilic polymer matrix. They possess both liquid- and solid-like characteristics. While these materials do not flow, they are very soft and allow the free diffusion of solutes. Furthermore, the high water content usually leads to biocompatibility. Extensively studied over the past 50 years,¹ hydrogels find uses as superabsorbents^{2,3} (packing material in hygienic and baby diapers, media for water retention in agriculture and wastewater management), in medicine⁴ (vehicles for controlled drug delivery⁵ and as scaffolds for tissue engineering⁶), in biotechnology⁷ (matrices for enzyme immobilization and media for electrophoresis), as soft contact lenses,⁸ and in sensors and actuators.⁹

Amphiphilic polymer conetworks (APCNs), first reported in 1988 by Kennedy¹⁰ and Stadler,¹¹ are related to hydrogels and have received increased attention in the past 10–15 years.¹² APCNs are composed of covalently interconnected hydrophilic and hydrophobic segments, swell in both polar and nonpolar solvents, and can solubilize both polar and nonpolar solutes. Furthermore, the arrangement of each type of units in relatively long sequences results in APCN self-assembly in selective solvents, very much like the micellization of conventional low-molecular-weight surfactants and linear amphiphilic block copolymers, and the creation of a large interfacial area.¹³ This internal self-organization differentiates APCNs from simple hydrogels and enables them for use in niche applications, e.g., as materials in antifouling coatings,¹⁴ modern soft contact lenses,¹⁵

matrices for phase transfer reactions used in bio- and organocatalysis, and the fabrication of gas and optical sensors.¹⁶ APCNs may also have advantages over conventional hydrogels when used as matrices for controlled drug delivery.¹⁷

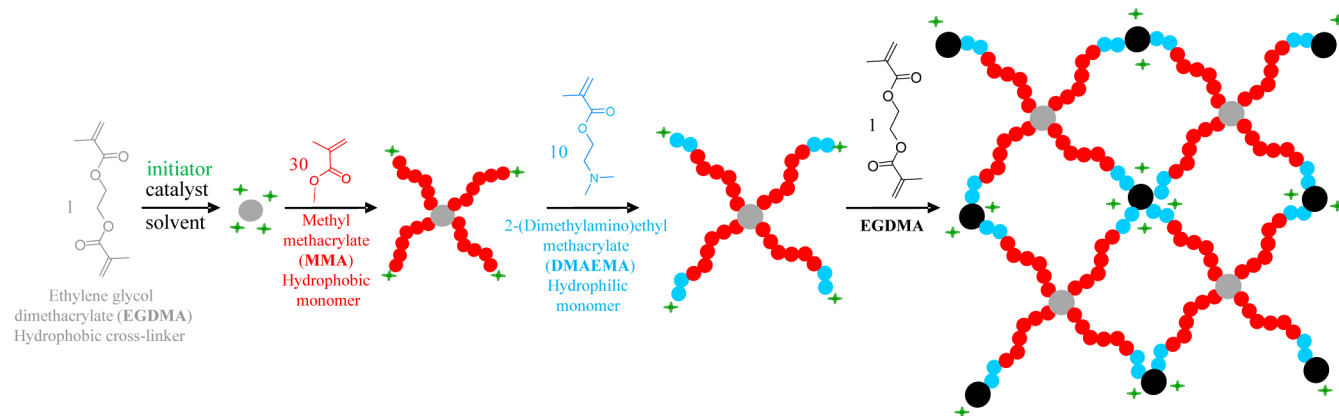
The cross-linked nature of APCNs implies some special characteristics for their microphase separation: First, chain relaxation and equilibration are slow compared to those of non-network polymer systems (linear and star copolymers), and second, unavoidable loops and chain entanglements¹⁸ lead to the entrapment of individual segments in domains of opposite philicity, compromising nanodomain purity. These explain why all experimentally studied APCNs exhibit incompletely separated nanophases with blurred interfaces,¹⁹ in spite of theoretical studies that predict APCN phase behavior similar to that of their linear block copolymer counterparts.²⁰ APCN phase separation with long-range order is challenging, and its achievement would endow these materials with superior properties, making them more efficient in their applications. To assist with APCN self-organization, we have been preparing these materials through a “block copolymer” approach, rather than the conventional “macro-cross-linker”²¹ or “hyperbranched core”²² approaches. Until now, morphologies with only short-

Received: August 26, 2015

Accepted: September 22, 2015

Published: October 1, 2015

Scheme 1. Schematic Representation of the Procedure Followed for Conetwork Preparation via Sequential Polymerization



range order have been obtained, as evidenced by scattering and microscopy measurements.²³

Herein, we report a one-pot preparation of APCNs that self-organize in lamellae with long-range order, as evidenced by microscopy and scattering. To the best of our knowledge, this is the first cross-linked polymer system that internally assembles with such high regularity. Subsequent characterization of the mechanical properties of the prepared APCNs revealed a positive correlation between structural order and mechanical strength, suggesting a clear advantage of the better ordered materials for use in practical applications.

The APCNs were prepared in the disordered state in tetrahydrofuran (THF), by the one-pot sequential group transfer polymerization²⁴ (GTP, a type of oxyanionic polymerization) of cross-linker (ethylene glycol dimethacrylate, EGDMA), hydrophobic comonomer (methyl methacrylate, MMA), hydrophilic comonomer (2-(dimethylamino)ethyl methacrylate, DMAEMA), and again cross-linker, as illustrated in Scheme 1. The chemical structures of the polymerization initiator and catalyst are given in Figure S1 in the Supporting Information. A “core-first” amphiphilic star block copolymer was produced after the third step of the synthetic procedure, which was end-linked at the final addition step, yielding the APCN.

Different comonomer feed ratios allowed the synthesis of APCNs with three different compositions, 25, 50, and 75 mol % MMA, whereas application of the two possible orders of comonomer addition gave rise to isomeric APCNs based on AB or BA star block copolymers, resulting in a total of six APCNs (for a list of all samples see Table S1). The structures of the star block copolymer precursors to these APCNs, along with those of the two “core-first” homopolymer star networks which were also prepared, are illustrated schematically in Figure S2 in the Supporting Information. The synthesis of “core-first” star polymers is well-documented in the literature,²⁵ whereas the synthesis of “core-first” star APCNs only recently appeared in a report where the focus was more on swelling measurements and model drug delivery rather than on morphology characterization.²⁶ APCNs based on amphiphilic “arm-first” star copolymers have been prepared by our group,²⁷ but scattering and microscopy characterization indicated self-assembly with only short-range order.²⁸

The “core-first” synthesis method used resulted in highly heterogeneous cores because, for the 1:1 cross-linker (EGDMA) to initiator (MTS) molar ratio employed, EGDMA could react with both other EGDMA molecules and initiator, producing a plethora of species (MTS₂-EGDMA₂₋₅, MTS₃-EGDMA₂₋₈,

MTS₄-EGDMA₅₋₈, and MTS₅-EGDMA₈₋₁₃), identified using MALDI-TOF, and presented in Figure S4. The molecular weight distributions (MWDs) of the cores and the star (co)polymers were trimodal (recorded using gel permeation chromatography, GPC, Figure S3), with very high molecular weight dispersities, \mathcal{D} , for the cores (~ 5.0) and notably lower for the star polymers (~ 2.5) (Table S1); the better size homogeneity of the star polymers compared to that of their parent cores can be attributed to the well-defined size of the produced arms, in combination with the reduced (due to arm steric hindrance) coupling between the cores of the star polymers. The relative number-average molecular weights, M_n , of the star polymers were ca. 20 kDa, with the relative peak molecular weights, M_p , of the largest star polymers (peaks on the left of the chromatograms) being around 80 kDa; however, the absolute M_w values, determined using static light scattering, were much larger, 885 kDa, corresponding to an average arm number of 206. Note that the polydispersity in star size arises from the broad distribution in arm number rather than in arm length. Thus, the star polymer precursors to the APCNs were large but also heterogeneous in size.

All APCNs swelled in a pH-dependent fashion, exhibiting increased swelling below pH 7, a result of the ionization of the hydrophilic, pH-responsive DMAEMA²⁹ units (Figure S5). The swelling results are summarized in Figure S6, where the aqueous swelling degrees at full and zero ionization of the DMAEMA units are given; higher swelling is observed at higher ionization and for APCNs richer in the hydrophilic DMAEMA units, as expected.

The self-organization of the APCNs in the dried and the water- or D₂O-swollen states was investigated using atomic force microscopy (AFM) and small-angle neutron scattering (SANS), respectively, whereas the presence of anisotropic phases in the water-swollen conetworks was examined via polarized light microscopy. Figure 1 shows the results for sample EGDMA₁-b-MMA₃₀-b-DMAEMA₁₀-b-EGDMA₁. This sample exhibits self-assembly with the longest-range order, whereas the results for all samples are displayed in the Supporting Information in Figures S7–S12. Figure 1(a) shows the AFM image of the particular sample equilibrated in water; before its transfer to water, the sample was annealed overnight in a vacuum oven at 105 °C, a temperature above the T_g of PMMA, in order to allow the PMMA segments to equilibrate (the T_g of the PDMAEMA segment is much lower, 0–20 °C). The AFM image displays lamellae with long-range order and lamellar period thickness of about 20 nm, in good agreement with the molecular dimensions

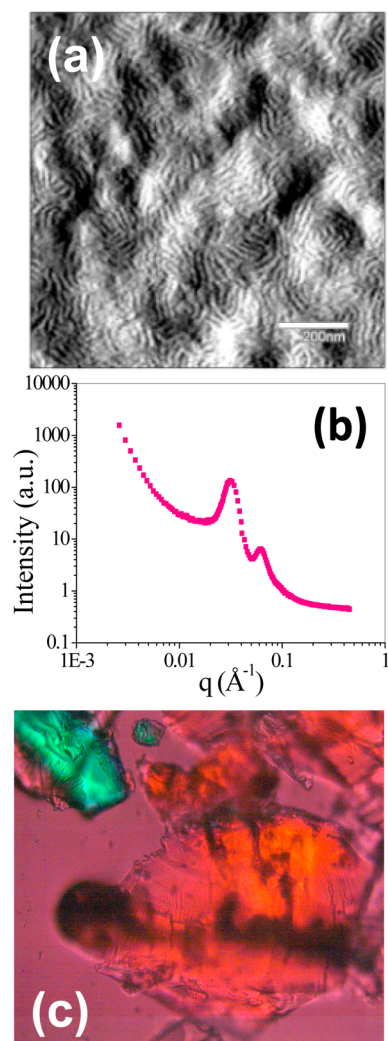


Figure 1. Structure formation with long-range order exhibited by sample EGDMA₁-*b*-MMA₃₀-*b*-DMAEMA₁₀-*b*-EGDMA₁ in water, as observed using (a) AFM (phase mode), (b) SANS, and (c) polarized light microscopy, with image dimensions 625 $\mu\text{m} \times 625 \mu\text{m}$.

of the arms of the star copolymer (contour length of 10.1 nm = 40 units \times 0.252 nm/unit; lamellar thickness indeed comes out to be ca. twice the contour length, indicating stretched chains, as expected for multiarm star polymers). Figures S7 and S8 show the AFM images of all samples in bulk before and after thermal annealing, respectively.

Figure 1(b) presents the SANS profile of the same sample after thermal annealing, equilibrium-swollen in D₂O. The SANS curve exhibits a double peak, with the minor peak located at a q -value exactly twice that of the major peak, indicative of a lamellar morphology with a long-range ordering. The lamellar spacing between the scattering centers ($= 2\pi/q_{\text{max}}$) is 20 nm (Table S2), in excellent agreement with the AFM results. To our knowledge, this is the first well-defined morphology observed with APCNs synthesized and cross-linked in the disordered state. It is also noteworthy that the composition of the particular APCN sample (33 wt % DMAEMA, calculated from the molar composition of 24 mol % DMAEMA determined using ¹H NMR spectroscopy on the star block precursor) correctly corresponds to lamellae.^{20f}

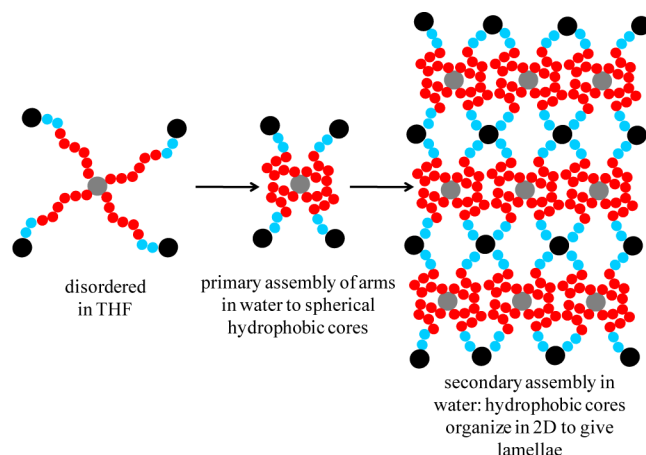
The SANS profiles of all the APCNs in D₂O were recorded both before and after thermal annealing in the solid state (Figures S9 and S10), and the respective results are similar, with

only some slight sharpening of the minor peak after thermal treatment. Thus, we may conclude that the self-assembly of APCNs in a selective solvent, such as water, is readily driven close to equilibrium without the need for thermal annealing.

Figure 1(c) displays the image of the water-swollen sample under a polarized light microscope. The image of this sample exhibited the most intense color variation (birefringence) from all APCN samples, in agreement with the SANS results, and confirming its organization in a liquid crystalline lamellar phase. The coloration clearly comes from the bulk of the ground particles and not from reflections from surface planes cut at irregular ways. Note that birefringence results from at least one of the nanophases exhibiting refractive indices which are different in different directions. The two homopolymers did not display any color variation, as expected (Figure S11).

Scheme 2 illustrates the steps for structure formation within the APCN from the arrangement of its constituting star block

Scheme 2. Hierarchical Internal Organization of the Building Blocks of the Amphiphilic Polymer Conetwork to Lamellae



copolymer units. The amphiphilic star block copolymer cell is initially in a swollen-disordered state upon its synthesis in the nonselective organic solvent. However, when transferred into water, it forms a hydrophobic core via the assembly of the inner hydrophobic blocks around the primary cross-linking core. Furthermore, these hydrophobic cores further assemble in two dimensions to form the lamellar morphology. These two levels of organization probably do not take place sequentially, but most likely simultaneously.

We believe that several factors facilitate this well-ordered organization, despite the broad distribution in arm numbers, the relatively low molecular weights of the arms, and the low incompatibility between the hydrophilic and hydrophobic monomer repeating units. First, the very high molecular weight of the building blocks, the star copolymers, provides a strong driving force for microphase separation; moreover, since these large block copolymers are prepared first, and then interconnected to give the network, this helps minimize chain entanglements. Second, the homogeneity in the size and composition of the arms favors a high order in the resulting structure. Third, the preorientation of the arms (all red blocks cross-linked at the gray core and all blue blocks held at a black core) and their large number per core facilitates the attainment of equilibrium. Fourth, the relatively low cross-linking density (low dose of EGDMA cross-linker, equally distributed between the first and fourth addition steps) maintains high segment

mobility, allowing the chains to readily relax to the equilibrium state of minimum free energy. Finally, the modest swelling degree, conferred upon the conetwork by its high hydrophobicity, helps hide structural defects, whose presence would become apparent upon further swelling and stretching. It might, therefore, not be a coincidence that the morphology with the long-range order obtained was the lamellar, as this morphology is characterized by the lowest curvature and the minimum (asymmetric) chain stretching.

One may ask the question why the isomeric structure with the inverse arm architecture, DMAEMA₁₀-*b*-MMA₃₀ as compared to MMA₃₀-*b*-DMAEMA₁₀, did not result in a morphology with long-range order. The discrepancy may be related to the different numbers of arms emanating from the two types of cores, the primary (in gray) and the secondary (black). Our previous investigations³⁰ indicated that the secondary cores bear fewer arms than the primary. We may expect a more efficient self-assembly when the insoluble block emanates directly from the core with greater functionality. This indeed appears to be the case, with the MMA₃₀-*b*-DMAEMA₁₀ isomer exhibiting longer-range order.

Next, we characterized the mechanical properties of the APCNs³¹ in compression, which are relevant to all potential applications. Figure 2 presents the compressive stress at break

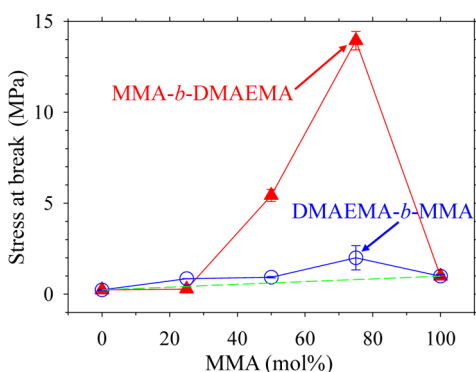


Figure 2. Ultimate compressive stress of all developed networks swollen in water.

for all six APCNs, together with those for the two homopolymer star networks, swollen in water, whereas Figure S12 displays the compressive strain at break and the low-strain (~10%) Young's modulus. The dashed green straight line in the bottom of the plot in Figure 2 interconnects the points corresponding to the two homopolymer networks and represents the expected stress at break values of the APCNs, if a simple proportionality law is applied. The measured stress at break values for most APCNs lies above the dashed line, indicating a synergistic behavior. This synergy has also been observed for the tensile strength of linear block copolymers in the bulk, but its extent was much smaller.³² The stress at break for the best-ordered APCN, EGDMA₁-*b*-MMA₃₀-*b*-DMAEMA₁₀-*b*-EGDMA₁, is much higher than the proportionality law dictates, suggesting a very strong synergy, and indicating that the high structural regularity in this sample may provide a most efficient energy dissipation mechanism, possibly via thin-layer or "fibril" yielding.³³ The particular value of the compressive strength in this sample (~14 MPa) is very close to that of double-network hydrogels (~17 MPa)³⁴ which represent one of the most mechanically robust hydrogel systems developed to date.

To confirm the correctness of our results regarding the phase separation with long-range order within the particular APCN sample, the SANS characterization was repeated, resulting in essentially the same SANS profile clearly presenting a second-order peak (Figure S13(a)). Furthermore, the synthesis of the particular sample was repeated, and the new sample was characterized by SANS again, leading to a very similar SANS profile with a second-order peak (Figure S13(b)).

In summary, we have presented the first APCN hydrogel, based on cross-linked star block copolymers, self-organizing in water into a lamellar mesophase with long-range order, a behavior previously known only for non-cross-linked block copolymer systems. The mechanical properties of the well-ordered system are clearly superior to those of its homologues, which, together with the facile, one-pot preparation using readily available components, are expected to render the present system popular for applications in medicine and biotechnology.

■ ASSOCIATED CONTENT

📄 Supporting Information

The Supporting Information is available free of charge on the ACS Publications website at DOI: 10.1021/acsmacrolett.5b00608.

Experimental details on synthesis and characterization; molecular weights and compositions of network precursors; degrees of swelling, AFM images, SANS profiles, polarized light micrographs, compressive strain at break, and low-strain Young's modulus for all networks (PDF)

■ AUTHOR INFORMATION

✉ Corresponding Author

*E-mail: costasp@ucy.ac.cy.

Notes

The authors declare no competing financial interest.

■ ACKNOWLEDGMENTS

This work was cofunded by the European Regional Development Fund and the Republic of Cyprus through Cyprus Research Promotion Foundation (infrastructure projects IPE/NEKYP/0311/27 and 0308/02). We also acknowledge the European Research Council (ERC, grant 336839), neutron beam time at the Institut Laue-Langevin (ILL) Grenoble, France, the Jülich Center for Neutron Science (JCNS), Garching, Germany, and the National Institute of Standards and Technology (NIST), Gaithersburg, Maryland. Furthermore, we thank our colleagues Dr. Paul D. Butler (NIST), Dr. Ingo Hoffmann (ILL), and Dr. Marie-Sousai Appavou (JCNS) for their help with the SANS measurements and also Dr. Florian Johann (Asylum) for his help with the AFM measurements in water. Finally, we express our gratitude to our colleague Professor Yoshihito Osada of RIKEN, Wako, Saitama, Japan, for his valuable comments and suggestions for our work.

■ REFERENCES

- (1) Patrickios, C. S., Ed. *Polymer Networks: Synthesis, Properties, Theory and Applications*; Wiley-VCH: Weinheim, 2010; Vol. 291–292.
- (2) Buchholz, F. L.; Peppas, N. A., Eds. *Superabsorbent Polymers*; ACS Symposium Series; American Chemical Society: Washington, DC, 1995; Vol. 573.
- (3) Buchholz, F. L.; Graham, A. T., Eds. *Modern Superabsorbent Polymer Technology*; Wiley: New York, 1998.

- (4) Peppas, N. A.; Hilt, J. Z.; Khademhosseini, A.; Langer, R. *Adv. Mater.* **2006**, *18*, 1345–1360.
- (5) (a) Higginson, C. J.; Kim, S. Y.; Peláez-Fernández, M.; Fernández-Nieves, A.; Finn, M. G. *J. Am. Chem. Soc.* **2015**, *137*, 4984–4987. (b) Schmidt, J. J.; Rowley, J.; Kong, H. J. *J. Biomed. Mater. Res., Part A* **2008**, *87*, 1113–1122.
- (6) Drury, J. L.; Mooney, D. J. *Biomaterials* **2003**, *24*, 4337–4351.
- (7) Bailey, J. E.; Ollis, D. F. *Biochemical Engineering Fundamentals*, 2nd ed.; McGraw-Hill: Singapore, 1986.
- (8) Kopeček, J. *J. Polym. Sci., Part A: Polym. Chem.* **2009**, *47*, 5929–5946.
- (9) Calvert, P. *Adv. Mater.* **2009**, *21*, 743–756.
- (10) Chen, D.; Kennedy, J. P.; Allen, A. J. *J. Macromol. Sci., Chem.* **1988**, *A25*, 389–401.
- (11) (a) Weber, M.; Stadler, R. *Polymer* **1988**, *29*, 1064–1070. (b) Weber, M.; Stadler, R. *Polymer* **1988**, *29*, 1071–1078.
- (12) (a) Rikkou-Kalourkoti, M.; Patrickios, C. S.; Georgiou, T. K. In *Polymer Science: A Comprehensive Reference*; Matyjaszewski, K.; Möller, M., Eds.; Elsevier BV: Amsterdam, 2012; Vol. 6, pp 293–308. (b) Mespouille, L.; Hedrick, J. L.; Dubois, P. *Soft Matter* **2009**, *5*, 4878–4892. (c) Gitsov, I. *J. Polym. Sci., Part A: Polym. Chem.* **2008**, *46*, 5295–5314. (d) Erdodi, G.; Kennedy, J. P. *Prog. Polym. Sci.* **2006**, *31*, 1–18. (e) Patrickios, C. S.; Georgiou, T. K. *Curr. Opin. Colloid Interface Sci.* **2003**, *8*, 76–85.
- (13) Süvegh, K.; Domján, A.; Vankó, G.; Iván, B.; Vértés, A. *Macromolecules* **1998**, *31*, 7770–7775.
- (14) (a) The alternation of hydrophilic and hydrophobic (preferably fluorophilic) domains minimizes bacterial adsorption on to APCNs. (b) Krishnan, S. In *Polymer Adhesion, Friction, and Lubrication*; Zeng, H. B., ed.; Wiley: Hoboken, 2013. (c) Zhu, X.; Guo, S.; Jańczewski, D.; Parra Velandia, F. J.; Teo, S. L.-M.; Vancso, G. J. *Langmuir* **2014**, *30*, 288–296. (d) Detty, M. R.; Ciriminna, R.; Bright, F. V.; Pagliaro, M. *Acc. Chem. Res.* **2014**, *47*, 678–687. (e) Imbesi, P. M.; Finlay, J. A.; Aldred, N.; Eller, M. J.; Felder, S. E.; Pollack, K. A.; Lonnerker, A. T.; Raymond, J. E.; Mackay, M. E.; Schweikert, E. A.; Clare, A. S.; Callow, J. A.; Callow, M. E.; Wooley, K. L. *Polym. Chem.* **2012**, *3*, 3121–3131. (f) Siedenbiedel, F.; Fuchs, A.; Moll, T.; Weide, M.; Breves, R.; Tiller, J. C. *Macromol. Biosci.* **2013**, *13*, 1447–1455.
- (15) (a) In modern soft contact lenses, a hydrophilic nanophase secures softness and on-eye comfort; a polysiloxane or polyperfluoroether nanodomain imparts high oxygen permeability; and a glassy hydrophobic phase confers toughness and mechanical robustness; furthermore, a co-continuous phase morphology is essential for the desired contact lens mobility as opposed to adherence to the eye. (b) Nicolson, P. C.; Vogt, J. *Biomaterials* **2001**, *22*, 3273–3283.
- (16) (a) In matrices for phase transfer reactions, the substrate resides in one nanophase and the catalyst in the other. (b) Schoenfeld, I.; Dech, S.; Ryabenky, B.; Daniel, B.; Glowacki, B.; Ladisch, R.; Tiller, J. C. *Biotechnol. Bioeng.* **2013**, *110*, 2333–2342. (c) Hensle, E. M.; Tobis, J.; Tiller, J. C.; Bannwarth, W. *J. Fluorine Chem.* **2008**, *129*, 968–973. (d) Meskath, S.; Urban, G.; Heinze, J. *Sens. Actuators, B* **2013**, *186*, 367–373. (e) Hanko, M.; Bruns, N.; Tiller, J. C.; Heinze, J. *Anal. Bioanal. Chem.* **2006**, *386*, 1273–1283. (f) Bruns, N.; Tiller, J. C. *Nano Lett.* **2005**, *5*, 45–48.
- (17) (a) Iván, B.; Kennedy, J. P.; Mackey, P. W. U.S. Patent, 5,073,381, 1991. (b) Iván, B.; Kennedy, J. P.; Mackey, P. W. *ACS Symp. Ser.* **1991**, *469*, 194–202. (c) Iván, B.; Kennedy, J. P.; Mackey, P. W. *ACS Symp. Ser.* **1991**, *469*, 203–212.
- (18) Zhou, H.; Schön, E.-M.; Wang, M.; Glassman, M. J.; Liu, J.; Zhong, M.; Diaz Diaz, D.; Olsen, B. D.; Johnson, J. A. *J. Am. Chem. Soc.* **2014**, *136*, 9464–9470. (b) Zhou, H.; Woo, J.; Cok, A. M.; Wang, M.; Olsen, B. D.; Johnson, J. A. *Proc. Natl. Acad. Sci. U. S. A.* **2012**, *109*, 19119–19124. (c) Rosselgong, J.; Armes, S. P. *Polym. Chem.* **2015**, *6*, 1143–1149. (d) Rosselgong, J.; Armes, S. P. *Macromolecules* **2012**, *45*, 2731–2737. (e) Stanford, J. L.; Stepto, R. F. T.; Waywell, D. R. *J. Chem. Soc., Faraday Trans. 1* **1975**, *71*, 1308–1326. (f) Dutton, S.; Stepto, R. F. T.; Taylor, D. J. R. *Angew. Makromol. Chem.* **1996**, *240*, 39–57.
- (19) (a) Koda, Y.; Terashima, T.; Takenaka, M.; Sawamoto, M. *ACS Macro Lett.* **2015**, *4*, 377–380. (b) Koda, Y.; Terashima, T.; Sawamoto, M. *J. Am. Chem. Soc.* **2014**, *136*, 15742–15748. (c) Walker, C. N.; Bryson, K. C.; Hayward, R. C.; Tew, G. N. *ACS Nano* **2014**, *8*, 12376–12385. (d) Krumm, C.; Konieczny, S.; Dropalla, G. J.; Milbradt, M.; Tiller, J. C. *Macromolecules* **2013**, *46*, 3234–3245. (e) Hu, Z. K.; Chen, L.; Betts, D. E.; Pandya, A.; Hillmyer, M. A.; DeSimone, J. M. *J. Am. Chem. Soc.* **2008**, *130*, 14244–14252. (f) Scherble, J.; Thomann, R.; Iván, B.; Müllhaupt, R. *J. Polym. Sci., Part B: Polym. Phys.* **2001**, *39*, 1429–1436. (g) Iván, B.; Almdal, K.; Mortensen, K.; Johannsen, I.; Kops, J. *Macromolecules* **2001**, *34*, 1579–1585.
- (20) (a) Schmid, F. *Phys. Rev. Lett.* **2013**, *111*, 028303. (b) Longo, G. S.; Olvera de la Cruz, M.; Szleifer, I. *ACS Nano* **2013**, *7*, 2693–2704. (c) Karbarz, M.; Stojek, Z.; Patrickios, C. S. *Macromol. Theory Simul.* **2013**, *22*, 323–334. (d) Karbarz, M.; Stojek, Z.; Georgiou, T. K.; Patrickios, C. S. *Polymer* **2006**, *47*, 5182–5186. (e) Karbarz, M.; Stojek, Z.; Patrickios, C. S. *Polymer* **2005**, *46*, 7456–7462. (f) Georgiou, T. K.; Vamvakaki, M.; Patrickios, C. S. *Polymer* **2004**, *45*, 7341–7355. (g) Jarkova, E.; Lee, N.-K.; Vilgis, T. A. *J. Chem. Phys.* **2003**, *119*, 3541–3549. (h) Vamvakaki, M.; Patrickios, C. S. *J. Phys. Chem. B* **2001**, *105*, 4979–4986.
- (21) Bruns, N.; Scherble, J.; Hartmann, L.; Thomann, R.; Iván, B.; Müllhaupt, R.; Tiller, J. C. *Macromolecules* **2005**, *38*, 2431–2438.
- (22) Powell, K. T.; Cheng, C.; Wooley, K. L.; Singh, A.; Urban, M. W. *J. Polym. Sci., Part A: Polym. Chem.* **2006**, *44*, 4782–4794.
- (23) (a) Rikkou-Kalourkoti, M.; Loizou, E.; Porcar, L.; Matyjaszewski, K.; Patrickios, C. S. *Polym. Chem.* **2012**, *3*, 105–116. (b) Pafiti, K. S.; Loizou, E.; Patrickios, C. S.; Porcar, L. *Macromolecules* **2010**, *43*, 5195–5204. (c) Rikkou, M. D.; Loizou, E.; Porcar, L.; Patrickios, C. S. *Eur. Polym. J.* **2010**, *46*, 441–449. (d) Rikkou, M. D.; Loizou, E.; Porcar, L.; Butler, P.; Patrickios, C. S. *Macromolecules* **2009**, *42*, 9412–9421. (e) Hadjiantoniou, N. A.; Patrickios, C. S.; Thomann, Y.; Tiller, J. C. *Macromol. Chem. Phys.* **2009**, *210*, 942–950. (f) Triftaridou, A. I.; Loizou, E.; Patrickios, C. S. *J. Polym. Sci., Part A: Polym. Chem.* **2008**, *46*, 4420–4432. (g) Kali, G.; Georgiou, T. K.; Iván, B.; Patrickios, C. S.; Loizou, E.; Thomann, Y.; Tiller, J. C. *Langmuir* **2007**, *23*, 10746–10755. (h) Triftaridou, A. I.; Vamvakaki, M.; Patrickios, C. S. *Biomacromolecules* **2007**, *8*, 1615–1623. (i) Kali, G.; Georgiou, T. K.; Iván, B.; Patrickios, C. S.; Loizou, E.; Thomann, Y.; Tiller, J. C. *Macromolecules* **2007**, *40*, 2192–2200. (j) Domján, A.; Erdödi, G.; Wilhelm, M.; Neidhöfer, M.; Landfester, K.; Iván, B.; Spiess, H. W. *Macromolecules* **2003**, *36*, 9107–9114. (k) Iván, B.; Harszti, M.; Erdödi, G.; Scherble, J.; Thomann, R.; Müllhaupt, R. *Macromol. Symp.* **2005**, *227*, 265–273. (l) Bruns, N.; Tiller, J. C. *Macromolecules* **2006**, *39*, 4386–4394.
- (24) Group transfer polymerization (GTP) of methacrylates. See for example: (a) Webster, O. W.; Hertler, W. R.; Sogah, D. Y.; Farnham, W. B.; Rajanbabu, T. V. *J. Am. Chem. Soc.* **1983**, *105*, 5706–5708. (b) Dicker, I. B.; Cohen, G. M.; Farnham, W. B.; Hertler, W. R.; Laganis, E. D.; Sogah, D. Y. *Macromolecules* **1990**, *23*, 4034–4041. (c) Webster, O. W. *Adv. Polym. Sci.* **2003**, *167*, 1–34. (d) Raynaud, J.; Ciolino, A.; Baceiredo, A.; Destarac, M.; Bonnet, F.; Kato, T.; Gnanou, Y.; Taton, D. *Angew. Chem., Int. Ed.* **2008**, *47*, 5390–5393. (e) Fuchise, K.; Chen, Y.; Satoh, T.; Kakuchi, T. *Polym. Chem.* **2013**, *4*, 4278–4291. (f) Rikkou-Kalourkoti, M.; Webster, O. W.; Patrickios, C. S. In *Encyclopedia of Polymer Science and Technology*; Wiley: New York, 2013; Vol. 99, pp 1–17.
- (25) (a) Eschwey, H.; Hallensleben, M. L.; Burchard, W. *Makromol. Chem.* **1973**, *173*, 235–239. (b) Gnanou, Y.; Lutz, P.; Rempp, P. *Makromol. Chem.* **1988**, *189*, 2885–2892. (c) Gao, H.; Matyjaszewski, K. *Macromolecules* **2008**, *41*, 1118–1125.
- (26) Ghasdian, N.; Church, E.; Cottam, A. P.; Hornsby, K.; Leung, M.-Y.; Georgiou, T. K. *RSC Adv.* **2013**, *3*, 19070–19080.
- (27) (a) Achilleos, D. S.; Georgiou, T. K.; Patrickios, C. S. *Biomacromolecules* **2006**, *7*, 3396–3405. (b) Vamvakaki, M.; Patrickios, C. S. *Chem. Mater.* **2002**, *14*, 1630–1638.
- (28) (a) Kafouris, D.; Gradzielski, M.; Patrickios, C. S. *Macromolecules* **2009**, *42*, 2972–2980. (b) Vamvakaki, M.; Patrickios, C. S.; Lindner, P.; Gradzielski, M. *Langmuir* **2007**, *23*, 10433–10437.
- (29) Iván, B.; Feldthausen, J.; Müller, A. H. E. *Macromol. Symp.* **1996**, *102*, 81–90.

- (30) Kafouris, D.; Themistou, E.; Patrickios, C. S. *Chem. Mater.* **2006**, *18*, 85–93.
- (31) Xu, J.; Bohnsack, D. A.; Mackay, M. E.; Wooley, K. L. *J. Am. Chem. Soc.* **2007**, *129*, 506–507.
- (32) (a) Weidisch, R.; Stamm, M.; Schubert, D. W.; Arnold, M.; Budde, H.; Höring, S. *Macromolecules* **1999**, *32*, 3405–3411. (b) Weidisch, R.; Michler, G. H.; Arnold, M.; Hofmann, S.; Stamm, M.; Jérôme, R. *Macromolecules* **1997**, *30*, 8078–8080.
- (33) (a) Michler, G. H.; Kausch, H. H.; Adhikari, R. *J. Macromol. Sci., Part B: Phys.* **2006**, *45*, 727–739. (b) Michler, G. H.; Adhikari, R.; Lebek, W.; Goerlitz, S.; Weidisch, R.; Knoll, K. *J. Appl. Polym. Sci.* **2002**, *85*, 683–700.
- (34) (a) Gong, J. P.; Katsuyama, Y.; Kurokawa, T.; Osada, Y. *Adv. Mater.* **2003**, *15*, 1155–1158. (b) Truong, V. X.; Ablett, M. P.; Richardson, S. M.; Hoyland, J. A.; Dove, A. P. *J. Am. Chem. Soc.* **2015**, *137*, 1618–1622.